Wannier-Stark states in double-periodic lattices. II. Two-dimensional lattices

Dmitrii N. Maksimov,[1] Evgeny N. Bulgakov,[1,2] and Andrey R. Kolovsky[1,3]
[1]*Kirensky Institute of Physics, 660036 Krasnoyarsk, Russia*
[2]*Siberian State Aerospace University, 660014 Krasnoyarsk, Russia*
[3]*Siberian Federal University, 660041 Krasnoyarsk, Russia*
(Received 25 November 2014; published 28 May 2015)

We analyze the Wannier-Stark spectrum of a quantum particle in tilted two-dimensional lattices with the Bloch spectrum consisting of two subbands, which could be either separated by a finite gap or connected by the Dirac points. For rational orientations of the static field given by an arbitrary superposition of the translation vectors, the spectrum is a ladder of energy bands. We obtain asymptotic expressions for the energy bands in the limit of large and weak static fields and study them numerically for intermediate field strength. We show that the structure of energy bands determines the rate of spreading of localized wave packets, which is the quantity measured in laboratory experiments. It is shown that wave-packet dispersion becomes a fractal function of the field orientation in the long-time regime of ballistic spreading.

DOI: 10.1103/PhysRevA.91.053632 PACS number(s): 03.75.Lm, 73.22.Dj, 05.60.Gg

I. INTRODUCTION

In the preceding paper [1] we have analyzed the Wannier-Stark (WS) states in a tilted one-dimensional (1D) double-periodic lattice. It was shown that the spectrum of WS states consists of two Wannier-Stark ladders that affect each other in a rather complicated way. In this paper we extend the analysis of Ref. [1] to double-periodic 2D lattices or, more exactly, to 2D lattices with two sublattices.

The fundamental difference of 2D lattices as compared with 1D lattices is that the WS spectrum and WS states depend not only on the strength of a static field F but also on its orientation relative to the primary axes of the lattice, where one should distinguish between rational and irrational orientations. The former are given by an arbitrary superposition of the translation vectors and the latter comprise the remaining directions. For rational orientations WS states are Bloch-like states in the direction orthogonal to the vector $\mathbf{F}$ [2–4]. Thus they can be labeled by the ladder index n and the transverse quasimomentum κ. Correspondingly, the energy spectrum of the system is a ladder of energy bands, which are termed WS bands in what follows. Unlike this situation, for irrational orientations the spectrum is pure point and WS states are localized states in any direction [4].

In the work we pay special attention to physical manifestations of the energy spectrum structure that can be detected in a laboratory experiment, where two favorite candidates are waveguide arrays [5] and cold atoms in optical lattices [6]. In particular, the continuous spectrum of the WS states for rational orientations of the static field implies ballistic spreading of a localized wave packet. This effect can be easily observed for the light in a waveguide array and, with some effort aimed at improving the resolution of the imaging system, for cold atoms in an optical lattice. We analyze the rate of wave-packet spreading as a function of the static field magnitude and its orientation. The other quantity that can be measured in experiments with cold atoms is the total occupation of the Bloch subbands, which changes in the course of time because of the interband Landau-Zener (LZ) tunneling. We show that knowing the WS spectrum, one can predict various regimes of the interband dynamics.

The structure of the paper is as follows. In Sec. II we introduce the model, the tight-binding Hamiltonian of a square 2D lattice with two sublattices, and perform a preliminary numerical analysis of the WS spectrum. In Sec. III we obtain asymptotic expressions for WS bands in the limits of strong and weak static fields. These results are used in Sec. IV, which compares the rate of ballistic spreading calculated on the basis of WS bands with that observed in numerical simulations of the wave-packet dynamics, and in Sec. V, which discusses Landau-Zener transitions between the Bloch subbands. The main results of the work are summarized in Sec. VI.

II. WANNIER-STARK ENERGY BANDS

In the second quantized form a quantum particle in a 2D lattice is described by the universal Hamiltonian

$$\widehat{H}_0 = \sum_{\mathbf{R}} \delta_{\mathbf{R}} \hat{c}^\dagger_{\mathbf{R}} \hat{c}_{\mathbf{R}} + \sum_{\mathbf{R},\mathbf{R}'} (J_{\mathbf{R},\mathbf{R}'} \hat{c}^\dagger_{\mathbf{R}'} \hat{c}_{\mathbf{R}} + \text{H.c.}), \qquad (1)$$

where the sum runs over all lattice sites located at the coordinates $\mathbf{R}$, $\delta_{\mathbf{R}}$ are the on-site energies, and $J_{\mathbf{R},\mathbf{R}'}$ are the hopping matrix elements between different sites. As the model we consider the square lattice of the unit period, which consists of two sublattices A and B (see Fig. 1). A quantum particle has on-site energies δ for the A sites and $-\delta$ for the B sites and can hop to the nearest sites with the tunneling rate J_1 (solid line bonds in Fig. 1) or J_2 (dashed line bonds). Notice that the primary axes of this lattice are rotated by 45° with respect to the xy axes and thus the new period is $a = \sqrt{2}$. We also mention that a cold-atom implementation of this model has recently been reported in Ref. [6].

Using the plane-wave ansatz for eigenfunctions of the specified Hamiltonian, the stationary Schrödinger equation $\widehat{H}_0 \psi(\mathbf{R}) = E\psi(\mathbf{R})$ reduces to the eigenvalue problem for the

2×2 matrix H_0,

$$H_0 = \begin{pmatrix} -\delta & -J_2 - J_1(e^{-i a\kappa_x} + e^{-i a\kappa_y} + e^{-i a(\kappa_x+\kappa_y)}) \\ -J_2 - J_1(e^{i a\kappa_x} + e^{i a\kappa_y} + e^{i a(\kappa_x+\kappa_y)}) & \delta \end{pmatrix}, \tag{2}$$

where κ_x and κ_y are the plane-wave quasimomenta. Two eigenvalues of the matrix (2) determine the Bloch spectrum of the system, consisting of two subbands with the dispersion relations $E = E_{\pm}(\kappa_x,\kappa_y)$. Correspondingly, eigenvectors of the matrix $[\psi_A(\kappa_x,\kappa_y),\psi_B(\kappa_x,\kappa_y)]^T$ determine the amplitudes of the Bloch wave for the A and B sites. Two particular cases to be considered in this work are (i) $J_1 = J_2$ and $\delta \neq 0$ and (ii) $\delta = 0$ and $J_2 = 0$. In relation to our preceding work [1] the former 2D lattice can be viewed as a coupled array of 1D lattices with alternating on-site energies and the latter 2D lattice is an array of 1D lattices with alternating tunneling elements. The Bloch spectra of lattices (i) and (ii) are shown in the left and right panels of Fig. 2, respectively. It can be seen in Fig. 2 that in case (i) two Bloch subbands are separated by a finite energy gap while in case (ii) they are connected by the Dirac cones. It appears that the absence or presence of the Dirac points in the Bloch spectrum strongly affects the WS spectrum and hence these two cases should be analyzed separately.

We proceed to the tilted lattices, where the Hamiltonian (1) should be complimented by the Stark term

$$\widehat{H} = \widehat{H}_0 + \sum_{\mathbf{R}} (\mathbf{F}\cdot\mathbf{R})\hat{c}^{\dagger}_{\mathbf{R}}\hat{c}_{\mathbf{R}}.$$

As it was already mentioned in Sec. I, the fundamental difference of tilted 2D lattices as compared with tilted 1D lattices is that the WS spectrum and WS states depend on the field orientation, which we characterize by the parameter $\beta = F_x/F_y$. Alternatively, one can characterize the field orientation by the parameter

$$\tilde{\beta} = \tilde{F}_x/\tilde{F}_y,$$

where $\tilde{F}_x$ and $\tilde{F}_y$ are field components in the coordinate system aligned with the primary axes of the lattice. Then rational orientations correspond to rational values of the parameter β, which also implies rational $\tilde{\beta} = r/q$ (here r and q are coprime numbers). An intuitive explanation for a qualitative difference between rational and irrational orientations follows from the observation that for a rational β we have equipotential lines of the lattice sites in the direction orthogonal to the field vector $\mathbf{F}$, while for irrational β the potential energies of all sites are strictly different. On the formal level this is reflected in the fundamentally different energy spectrum of WS states, which is discrete for irrational β and continuous for rational β.

To find the continuous energy spectrum for rational $\tilde{\beta} = r/q$ we follow Ref. [2] and rotate the coordinate system to align the new y axis with the vector $\mathbf{F}$ and then use the plane-wave ansatz for the wave function. This results in the eigenvalue problem

$$\begin{aligned} &dF\left(p - \frac{r+q}{4}\right)\psi^A_p + \delta\psi^A_p - J_2\psi^B_p \\ &\quad - J_1\left(e^{-ird\kappa}\psi^B_{p-q} - e^{iqd\kappa}\psi^B_{p-r} - e^{id(q-r)\kappa}\psi^B_{p-q-r}\right) \\ &\quad = E\psi^A_p, \\ &dF\left(p + \frac{r+q}{4}\right)\psi^B_p - \delta\psi^B_p - J_2\psi^A_p \\ &\quad - J_1\left(e^{ird\kappa}\psi^A_{p+q} - e^{-iqd\kappa}\psi^A_{p+r} - e^{-id(q-r)\kappa}\psi^A_{p+q+r}\right) \\ &\quad = E\psi^A_p, \end{aligned} \tag{3}$$

where the discrete index p is associated with different equipotential lines and

$$d = \frac{a}{\sqrt{N}}, \quad a = \sqrt{2}, \quad N = r^2 + q^2.$$

One obtains the WS bands through a sweep along the plane-wave quasimomentum κ that enters Eq. (3) as a parameter. As an example Fig. 3 shows these bands for the parameters of Fig. 2 and $F = 0.4$ and $(r,q) = (1,0)$. (In the original coordinate system this orientation corresponds to $F_x/F_y = 1$.) It can be seen in Fig. 3 that WS bands appear in pairs and are arranged into two ladders with steps dF. As F is varied the bands change their shape in a rather complicated way. On the other hand, if we fix the quasimomentum κ, we obtain the Wannier-Stark fan (see Fig. 4), which resembles that for a 1D double-periodic lattice. In particular, it can be seen in Fig. 4 that energy levels of different symmetry exhibit avoided crossings when they approach each other. If we now fix F and vary κ these avoided crossings become avoided crossings

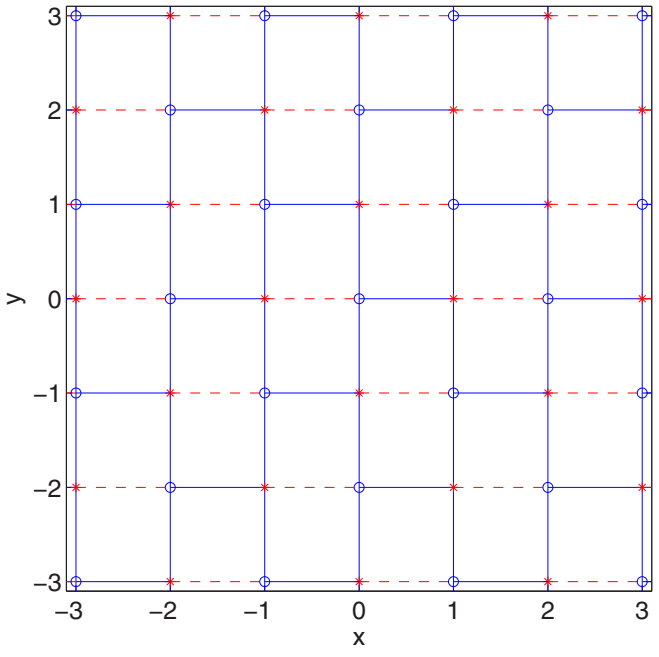

FIG. 1. (Color online) Tight-binding model. A quantum particle has on-site energies $\pm\delta$ for the A (open circles) and B (asterisks) sites and can tunnel out a given lattice site to the nearest site with the tunneling rate J_1 (solid line bonds) and J_2 (dashed line bonds).

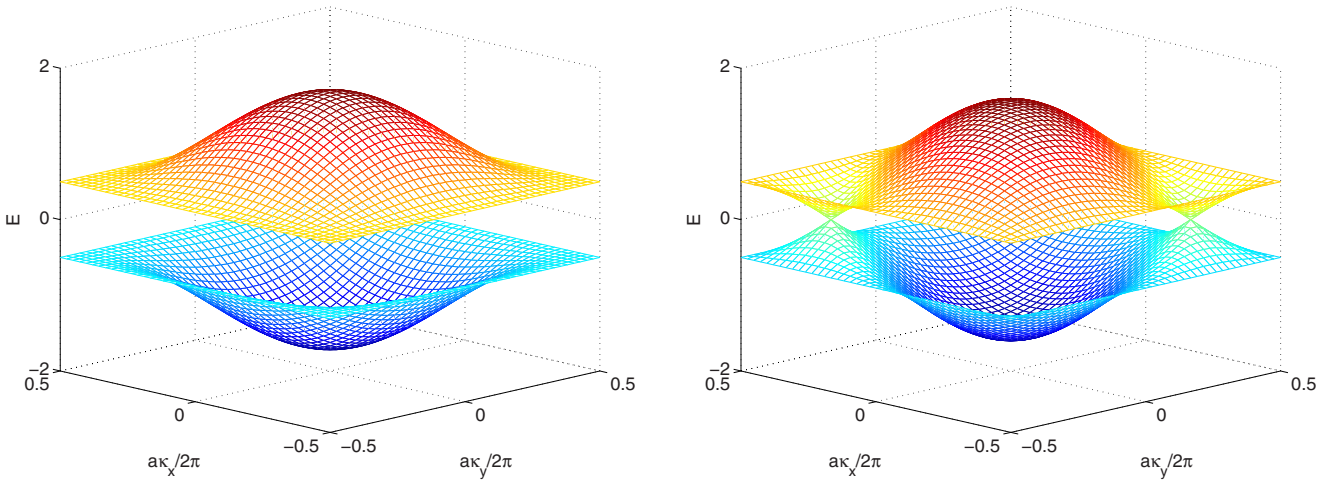

FIG. 2. (Color online) Bloch bands of the double-periodic lattice shown in Fig. 1 for $J_1 = J_2 = 0.4$ and $\delta = 0.5$ [lattice (i)] (left) and $J_1 = 0.5$ and $J_2 = \delta = 0$ [lattice (ii)] (right). The constants J_1, J_2, δ, and the energy E are measured in arbitrary energy units.

between energy bands. We would like to draw the reader's attention to the fact that the discussed avoided crossings are much more pronounced in case (ii); we return to this point in Sec. III C.

In the next section we analyze WS bands in more detail, focusing on their dependence on the static field F. Along with explicit form of the bands we are also interested in the mean-square group velocity

$$A(F) = \frac{1}{2\pi}\int_0^{2\pi} v^2(\kappa)d(d\kappa), \quad v(\kappa) = \frac{\partial E}{\partial \kappa}, \tag{4}$$

which is an important integral characteristic of WS bands. It will be shown later on in Sec. IV that the quantity (4) determines the rate of ballistic spreading of a localized wave packet. For the purpose of future reference Fig. 5 shows this quantity as the function of $1/F$.

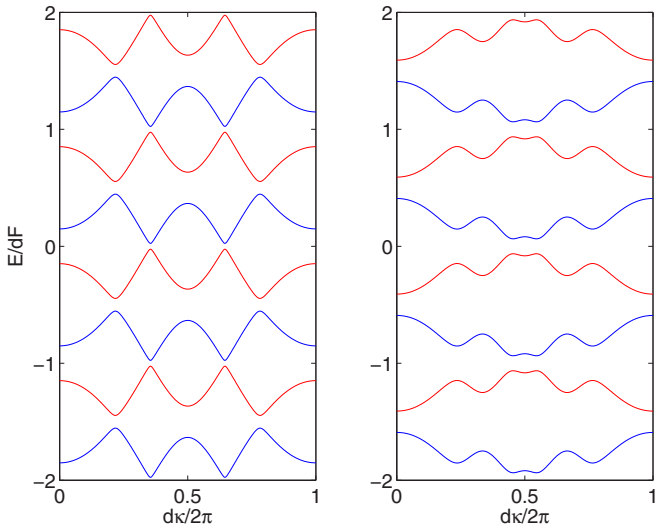

FIG. 3. (Color online) Ladders of Wannier-Stark energy bands for lattice (i) (left) and lattice (ii) (right). The parameters of the static field are $F = 0.4$ and $F_x/F_y = 1$.

III. STRONG VS WEAK FIELDS

A. Strong fields

The limit of strong fields can be solved using Rayleigh-Schrödinger perturbation theory with $\epsilon = 1/F$ as a small parameter. As follows from Eq. (3), the zeroth-order spectrum corresponds to flat bands arranged into two ladders. Denoting by $E^{(r,q)}(\kappa)$ the perturbation correction, we have

$$E_{n,\pm}(\kappa) = dF\left(n \mp \frac{r+q}{4}\right) \pm \delta \pm E^{(r,q)}(\kappa). \tag{5}$$

The superindex (r,q) in the correction term underlines its dependence on the field orientation. It can be rigorously proved that the few first terms in the perturbation series vanish and hence $E^{(r,q)}(\kappa) \sim \epsilon^{\nu}$, where ν is the number of vanishing terms. For example, for lattice (i) we have $\nu = 2$ if $F_x/F_y = 1$, $\nu = 3$ if $F_x/F_y = 1/3$, etc. Thus, in the general case the bandwidth Δ of the WS bands tends to zero if $F \to \infty$. Two exceptions, where the bands have a finite width in the above limit (i.e., $\nu = 0$), correspond to situations where **F** is aligned with the x or the y axis. It should be mentioned that the increment ν depends not only on the field orientation but also on the lattice geometry and for lattice (ii) we have $\nu = 0$ if **F** is parallel to the x axis and $\nu = 2$ if **F** is parallel to the y axis. It can be also shown that the first nonvanishing term of Rayleigh-Schrödinger perturbation theory gives the cosine dispersion relation for the WS bands

$$E^{(r,q)}(\kappa) = \Delta(F)\cos(Nd\kappa), \quad \Delta(F) \sim \frac{1}{F^{\nu}}. \tag{6}$$

Note that the dispersion relation $E^{(r,q)}(\kappa)$ is a periodic function of κ with the period $2\pi/Nd$ but not $2\pi/d$, as one might naively expect based on the explicit periodicity of the coefficients in Eq. (3). Finally, we mention that the functional dependence of the quantity (4) on F is obviously given by $A(F) \sim (1/F)^{2\nu}$ (see the inset in Fig. 5).

B. Moderate fields

The region of applicability of the common perturbation theory of Sec. III A is restricted to small values of the parameter

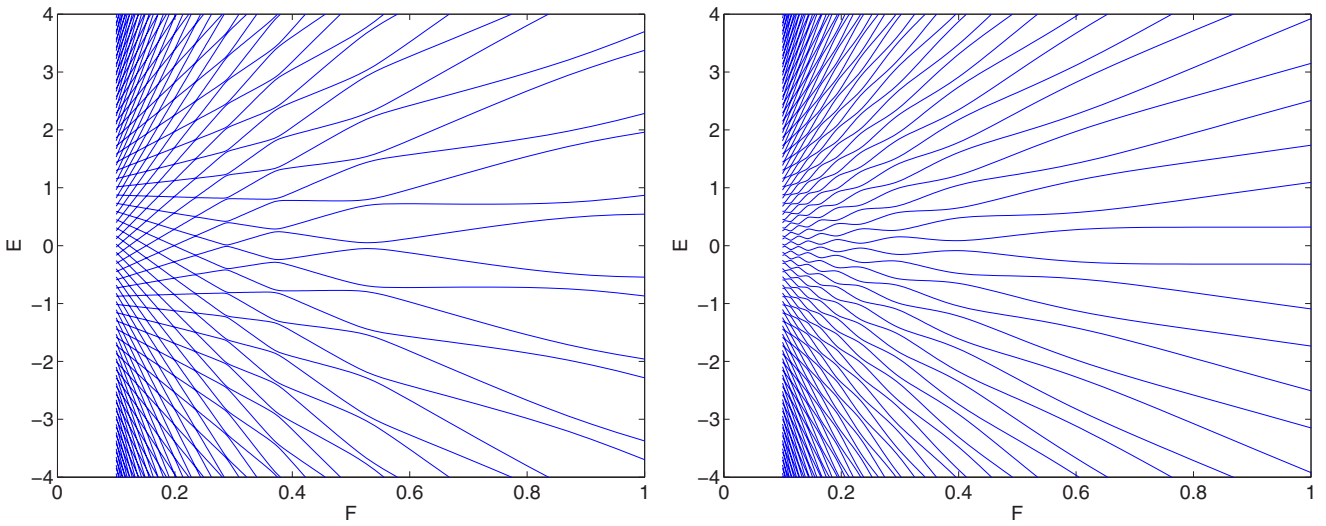

FIG. 4. (Color online) Wannier-Stark fans for lattice (i) (left) and lattice (ii) (right) for the field orientation $F_x/F_y = 1$. The transverse quasimomentum $\kappa = \pi/2d$, i.e., $d\kappa/2\pi = 0.25$.

$\epsilon = 1/F$, smaller than the position of the first peak in Fig. 5. In this section we discuss a more sophisticated approach that allows us to consider moderate F, where the bandwidth Δ of WS bands takes its maximal value. This approach is a straightforward generalization of the method used in Ref. [1] to analyze the WS spectrum of a quantum particle in 1D lattices.

Similar to Eq. (5) in Ref. [1] we introduce the generating functions

$$Y^{A,B}(\theta) = (2\pi)^{-1/2} \sum_{l=-\infty}^{\infty} \psi_l^{A,B} \exp(il\theta). \tag{7}$$

This reduces Eq. (3) to the system of two ordinary differential equations

$$idF \frac{d}{d\theta} \begin{pmatrix} Y^A \\ Y^B \end{pmatrix} = G(\theta;\kappa) \begin{pmatrix} Y^A \\ Y^B \end{pmatrix}, \tag{8}$$

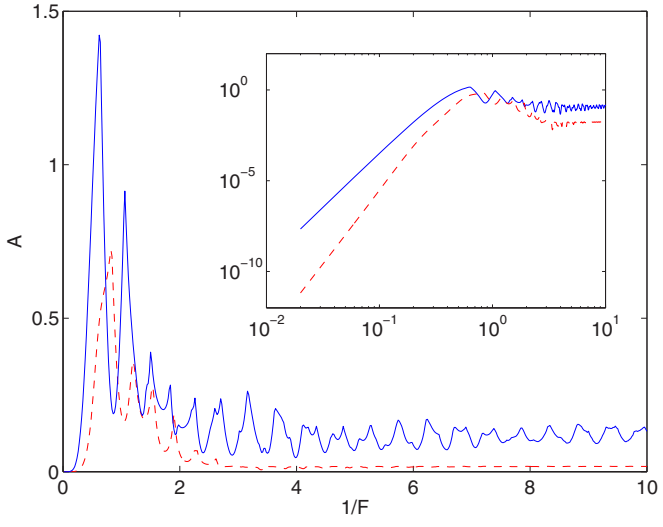

FIG. 5. (Color online) The quantity (4) as a function of $1/F$ for lattice (i) (dashed line) and lattice (ii) (solid line). The field orientation is $F_x/F_y = 1/3$ or $(r,q) = (2,1)$. The inset shows the same functions on a logarithmic scale.

where

$$G(\theta;\kappa) = \begin{pmatrix} E + dF(r+q)/4 + \delta & J_2 + J_1 f(\theta;\kappa) \\ J_2 + J_1 f^*(\theta;\kappa) & E - dF(r+q)/4 - \delta \end{pmatrix} \tag{9}$$

and

$$f(\theta;\kappa) = e^{-ird\kappa} e^{-iq\theta} + e^{iqd\kappa} e^{-ir\theta} + e^{i(q-r)d\kappa} e^{-i(r+q)\theta}.$$

Equation (8) falls into the class of linear dynamical systems and can be viewed as some effective two-level system driven by a three-chromatic field.

To solve Eq. (8) one can apply a variety of methods of which the Bogoliubov-Mitropolskii averaging technique proves to be the most universal [1]. For lattice (ii) this technique was used in our recent paper [7], from which we borrow the final result. Restricting ourselves by one iteration, the correction to the flat energy bands is given by

$$E^{(r,q)}(\kappa) = (J_2 - J_1) \sum_{n,m} \mathcal{J}_m(z_1)\mathcal{J}_n(z_2) \times \cos\left[\kappa d \frac{r^2+q^2}{r-q}(1+n)\right], \tag{10}$$

where the integer numbers n and m satisfy the equation $(r-q)m = -(r+q)(1+n)$ and the arguments of the Bessel functions are

$$z_1 = \frac{8J_1}{Fd(r-q)}, \quad z_2 = \frac{4(J_1+J_2)}{Fd(r+q)}.$$

Notice that, if compared with Rayleigh-Schrödinger perturbation theory, the first-order Bogoliubov-Mitropolskii correction corresponds to an infinite perturbation series.

Using the fact that $\mathcal{J}_n(z) \sim z^n$ for $z \ll 1$ it is easy to prove that in the limit $F \to \infty$ Eq. (10) recovers Eq. (6). However, unlike the former equation, Eq. (10) captures the oscillatory behavior of the bandwidth $\Delta = \Delta(F)$, as well as the presence of higher harmonics in the dispersion relation. For example, in the above-considered case $(r,q) = (2,1)$ Eq. (10) takes the

form

$$E^{(r,q)}(\kappa) = \pm(J_1 - J_2)[\mathcal{J}_0(z_1)\mathcal{J}_1(z_2) + \mathcal{J}_3(z_1)\mathcal{J}_0(z_2) \times \cos(5\kappa d) - \mathcal{J}_3(z_1)\mathcal{J}_2(z_2)\cos(5\kappa d) - \mathcal{J}_6(z_1)\mathcal{J}_1(z_2)\cos(10\kappa d) + \cdots]. \quad (11)$$

Comparing Eq. (11) with the exact numerical results, we found that for the parameters of Fig. 5 it correctly approximates WS bands until $F \approx 1$, where the quantity $A(F)$ has the first minima.

C. Weak fields

The opposite limit of small F is more involved in the sense that the result depends on the presence or absence of Dirac's points in the Bloch spectrum. First we discuss lattice (i), where the Bloch bands are separated by the gap equal to or larger than 2δ.

1. Finite gap

When discussing the case of small F it is convenient to think in terms of the time-dependent Schrödinger equation. In this picture the static field originates Bloch oscillations of a quantum particle in the Bloch subbands [see Eq. (15) below] and simultaneously induces interband LZ tunneling. A finite gap ensures vanishing interband LZ tunneling in the limit $F \to 0$. Thus the spectrum of 2D WS states can be found by using the adiabatic theorem, in full analogy with the weak-field case for 1D lattices [1]. Denoting by $\tilde{\mathcal{E}}_\pm(\theta;\kappa)$ and $\mathbf{y}_\pm(\theta;\kappa)$ the eigenvalues and eigenfunctions of the 2×2 matrix (9) for $E = 0$, the energy spectrum of WS states is given by the equation

$$E_{n,\pm}(\kappa) = C_\pm(\kappa) + dF[n + c_\pm(\kappa)], \quad (12)$$

where

$$C_\pm(\kappa) = \frac{1}{2\pi}\int_0^{2\pi} \tilde{\mathcal{E}}_\pm(\theta;\kappa)d\theta,$$
$$c_\pm(\kappa) = \frac{i}{2\pi}\int_0^{2\pi} \mathbf{y}_\pm^T(\theta;\kappa)\frac{d}{d\theta}\mathbf{y}_\pm(\theta;\kappa)d\theta' \quad (13)$$

are the dynamical and geometric phases, respectively. Equation (12) contains the transverse quasimomentum κ as a parameter. In fact, one can relate this quasimomentum and the constants (13) to the Bloch spectrum $E_\pm(\kappa_x,\kappa_y)$ of the system. To do this we rotate the axis in the quasimomentum space to align the new κ_y' axis with the vector $\mathbf{F}$ of the static field. Then the transverse quasimomentum κ is associated with κ_x' and the constant $C_\pm(\kappa)$ coincide in the limit $F \to 0$ with the mean energy of the Bloch subbands along the line parallel to $\mathbf{F}$:

$$\lim_{F\to 0} C_\pm(\kappa) = \frac{1}{2\pi}\int_0^{2\pi} E_\pm(\kappa,\kappa_y')d(d\kappa_y') \equiv \pm E^{(r,q)}(\kappa). \quad (14)$$

Let us discuss the dispersion relation (14) in some more detail. The left panel in Fig. 6 shows this dispersion relation for three different orientations of the static field: $(r,q) = (1,0)$, $(r,q) = (1,1)$, and $(r,q) = (2,1)$. It can be seen that $E^{(r,q)}(\kappa)$ rapidly converges to a flat band when r and q are increased. A more elaborate numerical analysis shows that this convergence

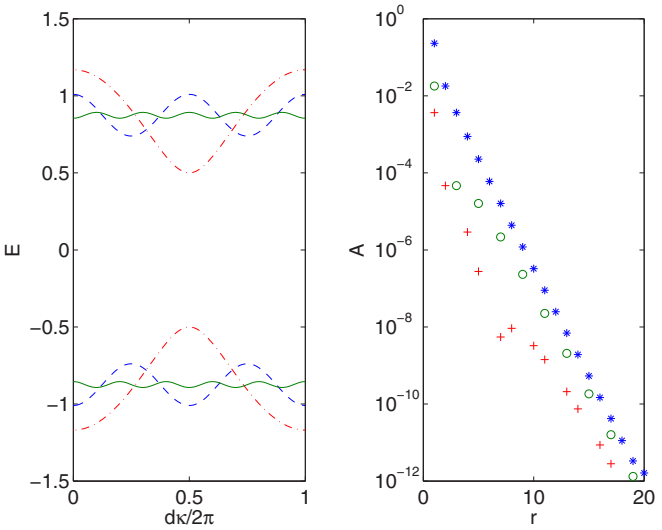

FIG. 6. (Color online) Shown on the left are the dispersion relations $E^{(r,q)}(\kappa)$ in the limit $F \to 0$ for lattice (i) and $(r,q) = (1,0)$ (dash-dotted line), $(r,q) = (1,1)$ (dashed line), and $(r,q) = (2,1)$ (solid line). Shown on the right is the quantity (4) calculated on the basis of the limiting dispersion relation for $1 \leqslant r \leqslant 20$ and $q = 1$ (asterisks), $q = 2$ (open circles), and $q = 3$ (pluses).

is exponentially fast (see the right panel in Fig. 6). Thus, for most of the field orientations the bandwidth Δ takes an exponentially small value in the limit $F \to 0$.

2. Dirac's cones

As can be seen in Fig. 5, for lattice (i) the quantity (4), which characterizes WS bands, takes a constant value as F is decreased. Obviously, this is a manifestation of the transition to the adiabatic regime of interband LZ tunneling. This result, however, does not hold for lattice (ii), where the Bloch subbands are connected by the Dirac points. In this situation we have non-negligible LZ tunneling for arbitrarily small F and arbitrary field orientations [8]. Correspondingly, the function $A = A(F)$ [Eq. (4)] does not take a constant value in the limit of small F.

To study the interband LZ tunneling we consider a delocalized initial condition given by a Bloch wave. For this initial condition the problem reduces to solving the Schrödinger equation

$$i\frac{d}{dt}\begin{pmatrix}\psi^A\\ \psi^B\end{pmatrix} = H(t)\begin{pmatrix}\psi^A\\ \psi^B\end{pmatrix}, \quad (15)$$

where $H(t)$ is obtained from the matrix (2) by substituting $\kappa_{x,y} \to \kappa_{x,y} - \tilde{F}_{x,y}t$. Notice that the solution depends on the initial quasimomenta. Thus, at any given time populations of the Bloch subbands are functions of κ_x and κ_y, i.e., $P_\pm(t) = P_\pm(\kappa_x,\kappa_y;t)$. Clearly, the interband dynamics also depends on the initial condition $P_\pm(\kappa_x,\kappa_y;t=0)$. In the work we consider two types of initial conditions: (a) $P_-(t=0) = \delta(\kappa_x)\delta(\kappa_y)$ and (b) $P_-(t=0) = \text{const}$ [in both cases $P_+(t=0) = 0$]. Physically, these initial conditions correspond to an ensemble of noninteracting Bose atoms at zero temperature and an ensemble of noninteracting Fermi atoms with the Fermi energy at $E = 0$ [6]. For this reason we refer to the just-specified

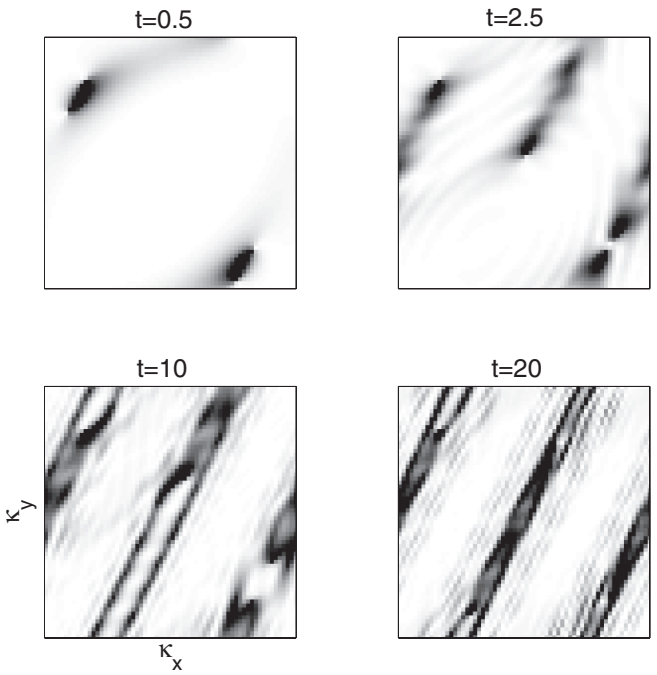

FIG. 7. Snapshots of $P_+(\kappa_x,\kappa_y;t)$ for lattice (ii) where initially the lower Bloch subband is completely populated. The parameters of the static field are $F = 0.2$ and $F_x/F_y = 1/3$. The time is measured in units of $T = 2\pi$. In a laboratory experiment this period is given by the ratio of Planck's constant to the chosen energy unit.

initial conditions as bosonic or fermionic. Figure 7 shows snapshots of $P_+(\kappa_x,\kappa_y;t)$ for lattice (ii) and the fermionic initial condition. It can be seen in the figure that the particles are transmitted into the upper band through the Dirac points. In addition to Fig. 7, Fig. 8 compares the time-averaged total populations of the upper band for lattices (i) and (ii). It can be seen that in the former case $\langle P_+\rangle \propto \exp(-1/F)$, while in the latter case $\langle P_+\rangle \propto$ const. This explains the qualitative difference between lattices (i) and (ii) in the weak-field limit.

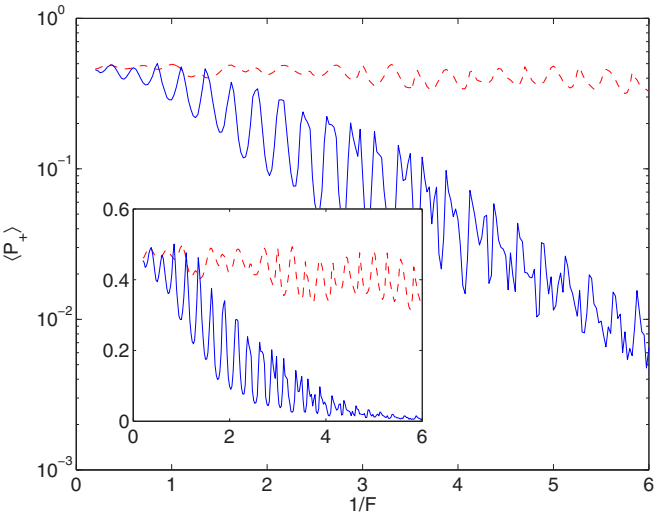

FIG. 8. (Color online) Time-averaged population of the upper band as a function of $1/F$ for lattice (i) (solid line) and lattice (ii) (dashed line) on linear (inset) and logarithmic (main panel) scales.

IV. BALLISTIC SPREADING OF A LOCALIZED WAVE PACKET

The continuous spectrum of WS states implies ballistic spreading of a localized wave packet where, asymptotically, the second moment of the packet grows quadratically in time:

$$M_2(t) \to Bt^2, \quad M_2(t) = \sum_{l,m}(l^2+m^2)|\psi_{l,m}(t)|^2.$$

For lattice (i) this behavior is illustrated in Fig. 9, where initially a single site at the lattice origin was populated. We mention that we will get essentially the same result if we choose a finite-width incoherent packet as the initial condition. Approximating numerical data in Fig. 9(a) by a straight line, we extract the coefficient B.

Let us now evaluate the second moment analytically. For simplicity we consider the case $(r,q) = (1,1)$, where the wave packet spreads in the x direction. Expanding the initial wave function over the basis of WS states, we obtain

$$\psi_{l,m}(t) = \sum_n \int d\kappa a_n(\kappa)\Psi_{l,m}^{(n,\kappa)} e^{-i[dFn+E(\kappa)]t}, \qquad (16)$$

where $a_n(\kappa)$ are the expansion coefficients and we omit the plus-minus index for two different WS ladders. Because WS states are Bloch-like states in the x direction, the following decomposition is valid: $\Psi_{l,m}^{(n,\kappa)} = b_m^{(n)}(\kappa)e^{i\kappa l}$. Next, using the identity $l\Psi_{l,m}^{(n,\kappa)} = -i\mathbf{b}_m^{(n)}(\kappa)de^{i\kappa l}/d\kappa$, one can prove the following intermediate result:

$$l\psi_{l,m} \approx t\sum_n \int d\kappa a_n(\kappa)\frac{\partial E}{\partial \kappa}\Psi_{l,m}^{(n,\kappa)} e^{-i[dFn+E(\kappa)]t}. \qquad (17)$$

To obtain this last equation we used integration by parts and kept only the term that grows in time. With the help of Eq. (17)

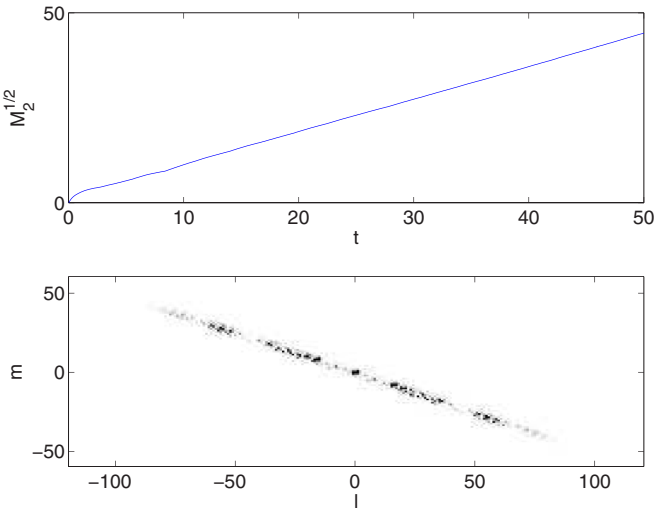

FIG. 9. (Color online) Shown on the top is the square root of the second moment as a function of time. Shown on the bottom are populations of the lattice sites $|\psi_{l,m}|^2$ at $t = 50T$. The parameters are lattice (i), $F = 0.8$, and $(r,q) = (2,1)$.

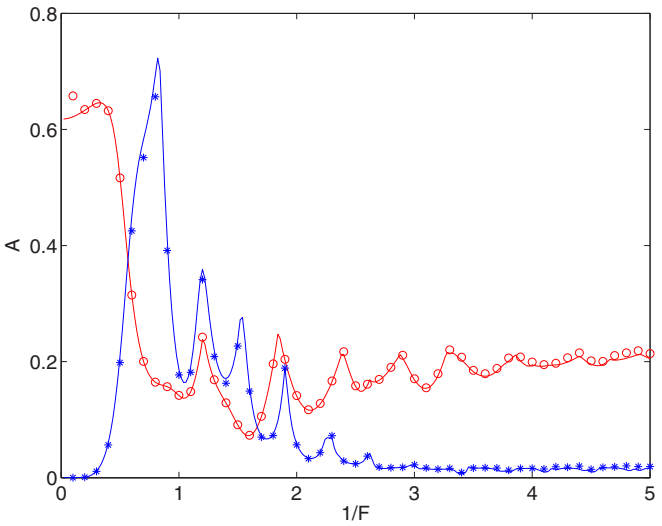

FIG. 10. (Color online) Rates of ballistic spreading as a function of $1/F$ (symbols) as compared to the analytic estimate (4) (solid lines). The field orientation is $F_x/F_y = 0$ (open circles) and $F_x/F_y = 1/3$ (asterisks).

the second moment is given by

$$M_2(t) \approx \sum_l |l\psi_{l,m}(t)|^2 = t^2 \sum_n \int d\kappa |a_n(\kappa)|^2 \left(\frac{\partial E}{\partial \kappa}\right)^2.$$

Finally, using the normalization condition $\sum_n \int d\kappa |a_n(\kappa)|^2 = 1$, we estimate the second moment as

$$M_2(t) \sim At^2, \tag{18}$$

where the coefficient A is defined in Eq. (4). Figure 10 compares the rate of ballistic spreading $B = B(F)$, which was obtained by using the wave-packet simulations, with the quantity $A = A(F)$, calculated from the dispersion relation of WS bands. Excellent agreement is noticed, in spite of a number of approximations that have been used to derive Eq. (18).

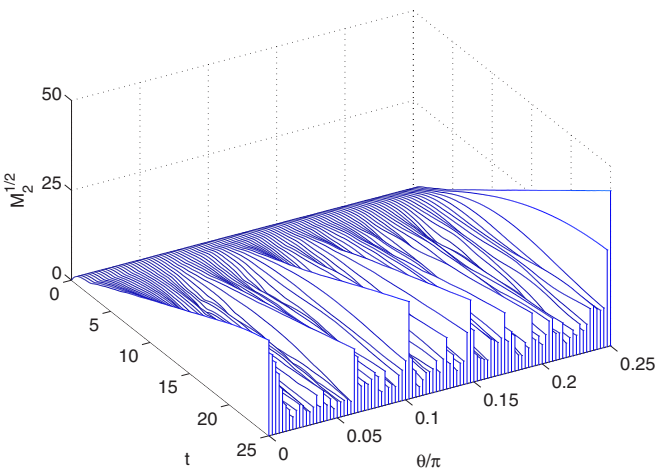

FIG. 11. (Color online) Dispersion $\sigma(t) = \sqrt{M_2(t)}$ as a function of time for several orientations of the static field $\theta = \arctan(F_x/F_y)$. The parameters are lattice (i) and $F = 0.8$.

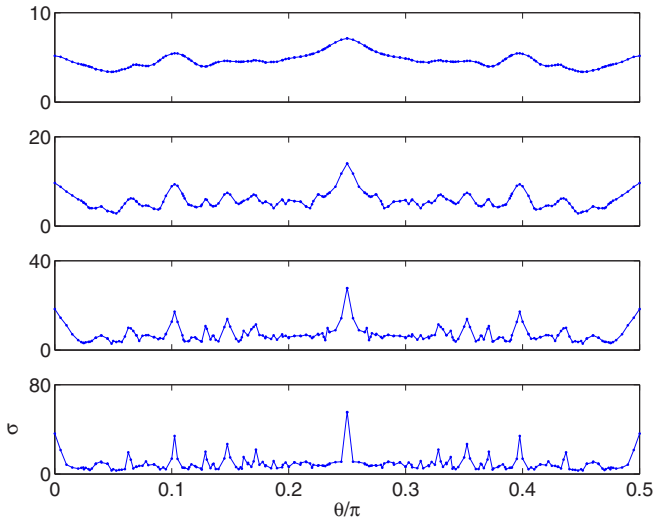

FIG. 12. (Color online) Dispersion $\sigma = \sigma(t;\theta)$ as a function of θ for four different times that differ by a factor of 2 for the nearest panels. Notice different upper limits for the vertical axis.

It is interesting to compare the wave-packet dispersion $\sigma(t) = \sqrt{M_2(t)}$ for different orientations of the vector $\mathbf{F}$ (see Fig. 11). In the considered case $F < J$ the short-time dynamics is defined by the ballistic spreading of a localized packet for $F = 0$. However, for longer times the system begins to experience the static field. At this stage it differentiates between rational and irrational orientations. For rational orientations the packet continues to spread in the direction orthogonal to the vector $\mathbf{F}$, while for irrational orientations dispersion $\sigma(t)$ saturates at some level. Considering the dispersion as a function of field orientation $\theta = \arctan(F_x/F_y)$, we observe the development of a fractal structure where each peak is associated with some rational $\beta = F_x/F_y$ (see Fig. 12).

V. INTERBAND DYNAMICS

As mentioned in Sec. I, cold atoms in optical lattices offer an opportunity for measuring population of the Bloch subbands. In this section we discuss population dynamics for the bosonic and fermionic initial conditions and relate it to the energy spectrum of WS states. On the formal level, the fermionic initial condition implies analysis of the population dynamics for arbitrary (not only zero) initial quasimomentum. Thus, if we consider, for example, the total population of the upper subband, the latter case involves the averaging of the solution of Eq. (15) over quasimomentum in the first Brillouin zone.

The thin solid lines in Fig. 13 show the total population of the upper Bloch band $P_+ = P_+(t)$ for the bosonic initial condition, where the two panels refer to rational orientation $F_x/F_y = 1/3$ and irrational $F_x/F_y = (\sqrt{5}-1)/4 \approx 1/3$. It can be seen that for the rational orientation $P_+(t)$ is (almost) periodic, while it is a complex quasiperiodic process for the irrational orientation. This is explained by the fact that the one-dimensional dispersion relation $E_\pm(t) = E_\pm(\kappa_x - \tilde{F}_x t, \kappa_y - \tilde{F}_y t)$, the quantity that implicitly enters the Schrödinger equation (15), is a periodic function of time for rational $\beta = F_x/F_y$ and a quasiperiodic function for irrational β. Thus,

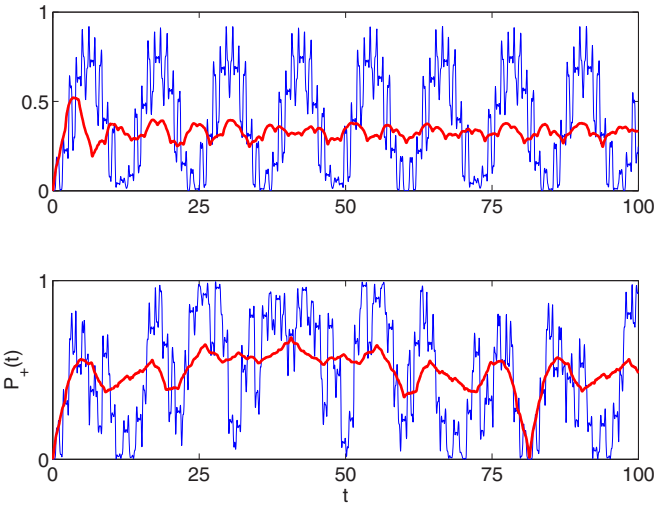

FIG. 13. (Color online) Total population of the upper subband as a function of time for $\beta = 1/3$ (top) and $\beta = (\sqrt{5}-1)/4 \approx 1/3$ (bottom). The thin and thick lines refer to the bosonic and fermionic initial conditions, respectively (see the text). The other parameters are lattice (i) and $F = 0.5$.

for rational β one can observe a periodic population dynamics, similar to periodic Stückelberg oscillations in one-dimensional lattices.

Remarkably, for the fermionic initial condition the situation is inverted. Because of the continuous spectrum of WS states for rational β, the averaging over the Brillouin zone leads to irreversible decay of oscillations, so the population of the upper band stabilizes at some level. In contrast, for irrational β the spectrum of WS states is discrete. As a consequence, the characteristic quasiperiod of $P_+(t)$ is the same for any initial quasimomentum and the averaging over the Brillouin zone reveals this quasiperiod [see the thick line in Fig. 13(b)].

VI. CONCLUSION

In the work we analyzed the energy spectrum of a quantum particle in tilted double-periodic lattices with square symmetry. It was shown that for rational orientations of a static field $\tilde{F}_x/\tilde{F}_y = r/q$, where r and q are coprime numbers, the spectrum consists of two ladders of energy bands termed Wannier-Stark bands. We obtained asymptotic expressions for the Wannier-Stark bands in the limit of strong and weak fields and numerically analyzed these bands for intermediate F.

As the main result we proved that the Wannier-Stark bands determine the rate of ballistic spreading of a localized wave packet, which is the quantity that can be directly measured in a laboratory experiment. Importantly, the spreading takes place only in the direction orthogonal to the vector **F**. The underlying phenomenon behind this effect is the interband Landau-Zener tunneling between Bloch subbands [9]. Thus the present work can be viewed also as an analysis of the interband Landau-Zener tunneling in 2D lattices, a problem that has attracted much attention in 1D lattices [10–16].

With respect to the wave-packet spreading, the results can be summarized as follows. In the strong-field limit the rate of ballistic spreading A obeys a universal law $A \sim 1/F^{\nu}$, where the increment ν is an integer number uniquely determined by the lattice geometry and the integers r and q. In the opposite weak-field limit the rate A also shows universal behavior provided the Bloch spectrum of the system does not contain Dirac points. If this is the case, A becomes independent of F and depends only on the lattice geometry and field orientation. In terms of Landau-Zener tunneling, these two asymptotic regimes correspond to nearly diabatic and adiabatic interband dynamics. For intermediate F the interband dynamics is neither diabatic no adiabatic and the rate A is a complicated function of the field magnitude, showing a number of peaks and dips. As argued in our recent paper [7], the oscillatory behavior of $A = A(F)$ is a two-dimensional analog of the phenomenon of dynamic localization in tilted and driven 1D lattices [17–19].

To avoid confusion, we would like to stress that we considered 2D lattices with the Bloch spectrum consisting of two subbands and all the above effects are absent in simple lattices with a single Bloch band. (Here "simple" does not imply simplicity of the Wannier-Stark problem; see Refs. [20,21], for example.) In the latter lattices the wave packet remains localized for any orientation of the vector **F**, excluding the trivial case where **F** is aligned with one of two primary axes of the lattice. In contrast to single-periodic 2D lattices, the wave packet in double-periodic 2D lattices spreads ballistically for every rational orientation $\theta = \arctan(r/q)$ with a well-defined rate $A = A(F,\theta)$. As a consequence, the wave-packet dispersion $\sigma = \sigma(\theta)$ develops a fractal structure in the course of time. This effect was predicted earlier in Ref. [22] for strongly decaying systems where the Wannier-Stark states are quantum resonances. Here we found it in not-decaying systems, which should facilitate its experimental observation.

ACKNOWLEDGMENT

The authors acknowledge financial support from Russian Foundation for Basic Research through the Project No. 15-02-00463, Wannier-Stark states and Bloch oscillations of a quantum particle in a generic two-dimensional lattice.

[1] D. N. Maksimov, E. N. Bulgakov, and A. R. Kolovsky, Wannier-Stark states in double-periodic lattices. I. One-dimensional lattices, preceding paper, Phys. Rev. A **91**, 053631 (2015).

[2] T. Nakanishi, T. Ohtsuki, and M. Saitoh, Stark ladders in two-dimensional tight-binding lattice, J. Phys. Soc. Jpn. **62**, 2773 (1993).

[3] M. Glück, F. Keck, A. R. Kolovsky, and H. J. Korsch, Wannier-Stark states of a quantum particle in 2D lattices, Phys. Rev. Lett. **86**, 3116 (2001).

[4] A. R. Kolovsky and E. N. Bulgakov, Wannier-Stark states and Bloch oscillations in the honeycomb lattice, Phys. Rev. A **87**, 033602 (2013).

[5] G. Corrielli, A. Crespi, G. Della Valle, S. Longhi, and R. Osellame, Fractional Bloch oscillations in photonic lattices, Nat. Commun. **4**, 1555 (2013).

[6] L. Tarruell, D. Greif, T. Uehlinger, G. Jotzu, and T. Esslinger, Creating, moving and merging Dirac points with a Fermi gas in a tunable honeycomb lattice, Nature (London) **483**, 302 (2012).

[7] E. N. Bulgakov and A. R. Kolovsky, Induced tunneling and localization for a quantum particle in tilted two-dimensional lattices, Phys. Rev. B **89**, 035116 (2014).

[8] L.-K. Lim, J.-N. Fuchs, and G. Montambaux, Bloch-Zener oscillations across a merging transition of Dirac points, Phys. Rev. Lett. **108**, 175303 (2012).

[9] A. R. Kolovsky and H. J. Korsch, Bloch oscillations of cold atoms in 2D optical lattices, Phys. Rev. A **67**, 063601 (2003).

[10] J. Rotvig, A.-P. Jauho, and H. Smith, Bloch oscillations, Zener tunneling and Wannier-Stark ladders in the time domain, Phys. Rev. Lett. **74**, 1831 (1995).

[11] D. W. Hone and X.-G. Zhao, Time-periodic behavior of multiband superlattices in static electric fields, Phys. Rev. B **53**, 4834 (1996).

[12] X.-G. Zhao, G. A. Georgakis, and Q. Niu, Rabi oscillations between Bloch bands, Phys. Rev. B **54**, R5235 (1996).

[13] B. Breid, D. Witthaut, and H. J. Korsch, Bloch-Zener oscillations, New J. Phys. **8**, 110 (2006).

[14] F. Dreisow, A. Szameit, M. Heinrich, T. Pertsch, S. Nolte, A. Tünnermann, and S. Longhi, Bloch-Zener oscillations in binary superlattices, Phys. Rev. Lett. **102**, 076802 (2009).

[15] S. Kling, T. Salger, C. Grossert, and M. Weitz, Atomic Bloch-Zener oscillations and Stückelberg interferometry in optical lattices, Phys. Rev. Lett. **105**, 215301 (2010).

[16] P. Plötz and S. Wimberger, Stückelberg-interferometry with ultra-cold atoms, Eur. Phys. J. D **65**, 199 (2011).

[17] X.-G. Zhao, Dynamic localization conditions of a charged particle in a dc-ac electric field, Phys. Lett. A **155**, 299 (1991).

[18] S. Longhi, M. Marangoni, M. Lobino, R. Ramponi, P. Laporta, E. Cianci, and V. Foglietti, Observation of dynamic localization in periodically curved waveguide arrays, Phys. Rev. Lett. **96**, 243901 (2006).

[19] A. Eckardt, M. Holthaus, H. Lignier, A. Zenesini, D. Ciampini, O. Morsch, and E. Arimondo, Exploring dynamic localization with a Bose-Einstein condensate, Phys. Rev. A **79**, 013611 (2009).

[20] F. Keck and H. J. Korsch, Infinete-variable Bessel functions in two-dimensional Wannier-Stark systems, J. Phys. A: Math. Gen. **35**, L105 (2002).

[21] A. Szameit, T. Pertsch, S. Nolte, A. Tünnermann, U. Peschel, and F. Lederer, Optical Bloch oscillations in general waveguide lattices, J. Opt. Soc. Am. B **24**, 2632 (2007).

[22] M. Glück, A. R. Kolovsky, and H. J. Korsch, Fractal stabilization of Wannier-Stark resonances, Europhys. Lett. **51**, 255 (2000).